

Measurements of the Three Dimensional Structure of Flames at Low Turbulence

M.R. Harker^a, M. Lawes^a, C.G.W. Sheppard^a, N. Tripathi^a and R. Woolley^b

^aSchool of Mechanical Engineering, University of Leeds
Leeds, United Kingdom

^bDepartment of Mechanical Engineering, University of Sheffield
Sheffield, United Kingdom

1. Introduction

Spark ignited flame kernels in a turbulence field do not immediately experience the full spectrum of turbulence scales present; initially they are wrinkled only by scales of smaller dimensions than the kernel, larger scales merely convecting them. Under nominally identical mean turbulence conditions, successive flame kernels behave differently, dependent upon the nature of the three dimensional turbulence adjacent to the ignition source from event to event. Not until the kernel becomes large enough and has existed long enough to encompass the bulk of scales available in the turbulent field, does the burn rate become consistent from shot to shot [1]. This is a major cause of cyclic variation in spark ignition (SI) engines and ignition variability in gas turbines. Slow burning mixtures are particularly affected and the phenomenon is an obstacle to the development of engines that yield low emissions or utilise lean burn or high exhaust gas recirculation (EGR).

The burning rate of such flames is often expressed in terms of a turbulent burning velocity (u_t), a parameter used in many thermodynamic cycle models of engine combustion and in explosion hazard assessment. However, measurement of u_t is problematic; particularly for flame kernels in their early stages of development, where it is necessary to quantify the turbulent scales affecting the flame at any instant and where these scales vary in 3-D and from explosion to explosion. Even the visualization and characterisation of 3-D solid objects is difficult, but in the case of a hot, transient and fluctuating flame surface the problem becomes extremely challenging. As a result, turbulent flames are typically visualised in 2-D using either laser sheets or an integrating technique such as shadowgraphy or schlieren imaging [2].

Combustion systems are routinely observed using a single 2-D sheet imaging techniques and this is especially effective in turbulent systems where it is possible to estimate the flame wrinkling [3], flame curvature [4] and reaction progress variables [5]. However 2-D laser sheet measurements reveal nothing about the flame in planes in front or behind the sheet. Movement of the flame kernel in the early stages of flame growth can result in flame displacement away from the laser sheet. Therefore, it is often impossible to determine whether the sheet is “slicing” through the centre of the flame kernel. To overcome such limitations of using single sheets, Yip et al. [6] used a laser beam which was

rapidly traversed through an aerosol seeded gas jet with the use of a rotating mirror. Images of different planes within the flow volume were recorded as the laser sheet swept through it. Since the images were successive rather than instantaneous, it was necessary that the traverse speed was very high relative to the flow movement between images.

The experiments reported here were designed to address the problems associated with single sheets by using a multiple sheet mie-scattered light technique to successfully characterise a non-stabilised expanding turbulent flame kernel in 3-D. A novel algorithm was developed to calculate turbulent flame parameters such as flame surface density (Σ), reaction progress variable (c) and the statistics of flame curvature from the 3-D flame structure.

2. Experimental Techniques

A 380 mm diameter spherical stainless steel vessel with extensive optical access through 3 pairs of orthogonal quartz windows of 150 mm diameter was employed. It could be operated at initial pressures and temperatures of up to 1.5 MPa and 600 K respectively. The windows provided the optical access for photographic and laser sheet techniques. The chamber was equipped with four identical, eight bladed fans to generate the turbulent flow field. These were symmetrically disposed in a regular tetrahedron configuration and directly coupled to an electric motor with separate speed control. The turbulent flow field was calibrated using laser doppler velocimetry (LDV) and particle image velocimetry (PIV) [7]. Measurements indicated that, within the optically accessed central region of 150 mm diameter, the turbulence was essentially isotropic with very low mean velocities. The rms turbulent velocity (u') was found to vary linearly with the fan speed. The turbulent integral length scale, L , was found directly from a spatial correlation to be 20 mm and was independent of all operating variables [7]. Lean turbulent methane-air flames were ignited in the centre of the vessel. The initial pressure and temperature were 0.1 MPa and 300 K respectively. The most successful seed for mie scattering was found to be olive oil with a typical diameter of 1.06 μm and a density of 970 kg/m^3 . This was introduced into the vessel using a TSI 9306 six jet atomiser.

Shown in Fig. 1 is the schematic diagram of the experiment. Laser sheet images were generated by an Oxford Lasers copper vapour laser LS20-50 capable of repetition rates from 2 KHz to 30 KHz. The pulse length was of the order of 20 ns and the pulse energy at 18 KHz, which was used throughout the present work, was typically 0.5 mJ. The laser beam was focussed using a plano-convex lens and a sheet generated with a plano-convex cylindrical lens. The laser sheet was moved using a rotating octagonal mirror. The speed of rotation was measured using a helium neon laser pointed towards the octagon mirror, a photo-diode was then positioned so that it detected the helium neon beam but not the copper vapour laser. There was a slight divergence between sheets, this was calculated to be less than 2 mm for the sheet at the images furthest from the spark.

The flame sheets were imaged with a Kodak Ektapro HS 4540 Motion Analyzer, which was used at 18,000 fps, with an image size of 255 * 64 pixels. A signal from the camera was used to synchronise the camera and laser. The chip had an effective film speed of 1600 ASA and was used in conjunction with a c-mount television lens with its aperture setting of f 1.1. The large aperture resulted in some image blurring in the sheets furthest from the spark gap where the camera was focussed, however, this was preferable to the reduction in contrast between burned and unburned gas if a smaller aperture was used. A 510 nm interference filter was placed between the laser sheet and the camera lens to filter out background light from the combustion event; this was particularly intense as a result of the emission of light from the seed as it heated.

Each face of the mirror generated one sweep through the combustion space with multiple laser firings (and images) per sweep. For a given laser repetition rate, the mirror speed determined both the sheet spacing and the number of sweeps through the combustion event. The lower the mirror speed the

closer the sheets but the lower the number of sweeps that could be recorded of the flame. Typically, a sweep took around 2 ms. Therefore it was important to select flames that were slow enough that they did not grow significantly during the time of sweep. A sheet height of approximately 50 mm was used. No attempt was made to synchronise the rotation of the mirror with the time of ignition in order to control the size of flame to be imaged. This was because the initial flame trajectory was found to be highly unpredictable, a result of the low laminar burning velocity (u_l) of the flame making it prone to convection by large turbulent scales.

3. Results and Discussion

Shown in Fig. 2 is a set of 25 laser sheet images, separated by 0.7 mm in the third dimension, through a flame kernel at an “instant”. The flame edge has been enhanced by a hand tracing technique resulting in the addition of a bright line so that the flame edge can be clearly identified. It can be seen that very little flame growth occurs in the time interval of 1.4 ms, covering the 25 images shown in Fig. 2. The spark plug is visible in the bottom left hand corner of the pictures and, in this combustion event, the kernel centroid can be seen to have migrated approximately “north north east”. This migration is a function of the larger scales of turbulence at the spark gap at the instant of ignition and is random from one combustion event to another. Sheets 1 and 25 cut through the flame kernel close to its outer edges, sheets 12-14 relate approximately to the centroid of the kernel, the spark gap is centred on sheet 13.

Viewed using schlieren photography, such kernels appear almost spherical, however, the multiple sheet images reveal considerable structure, even at this early stage of turbulent flame development. An apparent island of flame can be observed in Frames 17, 18 and 19, but this can be seen to interconnect with the main kernel in Frame 16. Similarly a pocket of mixture appears inside the flame in Frames 9 and 10; this is seen connected with the outside unburned gas in Frame 8. Unless very high turbulent levels have been achieved these islands and pockets are usually connected to the rest of the flame front. The resolution of approximately 0.7 mm in all three dimensions is reasonable when compared with the integral length scale of turbulence which is 20 mm. It is adequate to resolve structures that are of the order of the Taylor scale (3 mm) but not those of the order of the Kolmogorov scale (0.15 mm).

In order to regenerate an image of the full 3-D flame, the raw images were binarised, meshed and smoothed. The binarising process was performed in a number of stages. The last image prior to one containing the flame was used as a background image to obtain the initial image brightness. The background image was then subtracted from the successive individual images in turn, leaving only the flame present. A threshold value was then applied resulting in a black flame surrounded by white. The series of binary images were then processed by a computer program written in Matlab to construct a 3-D matrix, which was then isosurfaced. Such a reconstructed flame, however, was smoothed to remove surface imperfections like flat areas and square edges created by the individual sheets. An algorithm suggested by Taubin [8], which maximised smoothing and minimized shrinkage of the shape, was implemented. Figure 3 shows a typical image of a reconstructed and smoothed flame.

Having a fully reconstructed 3-D flame allowed for the accurate calculation of a range of flame parameters, such as flame curvature, flame surface area, reaction progress variable and flame surface density. Shown in Fig. 4 is a typical variation of average value of normalised flame surface density, $\Sigma\delta_l$, with normalised radius, r/L , at different times after ignition. Here, δ_l and r are the laminar flame thickness and radius from the instantaneous flame centroid respectively. It is observed that the profile width and peak value of $\Sigma\delta_l$, increase and decrease respectively with r/L at increasing time from ignition, implying an increase in flame thickness. This increase in flame thickness as the flame develops is more directly a function of flame size than of turbulence because an increase in flame size increases the surface area for the turbulence to act on, leading to an increase in flame wrinkling. Gashi et al. [9] used 3-D DNS to arrive at a similar conclusion.

4. Conclusions

Flames have been successfully mapped in 3-D using mie scattering images. A spatial resolution of 0.7 mm in both the images and in the third dimension separating adjacent sheets was achieved; this was adequate to resolve turbulent features to the Taylor scale for the experiment. A single turbulent flame kernel was “sliced” by 25 laser sheets. Novel computer algorithms were developed that process the laser sheet data to reconstruct the single sheets into a full 3-D flame allowing calculation of parameters that have previously been unobtainable for actual 3-D flames. The difference in both sheet images and 3-D reconstructions shows how different explosions and flames can be for the same conditions, and qualitatively gives an idea of why cycle to cycle variation can have different effects on the flame.

5. Figures

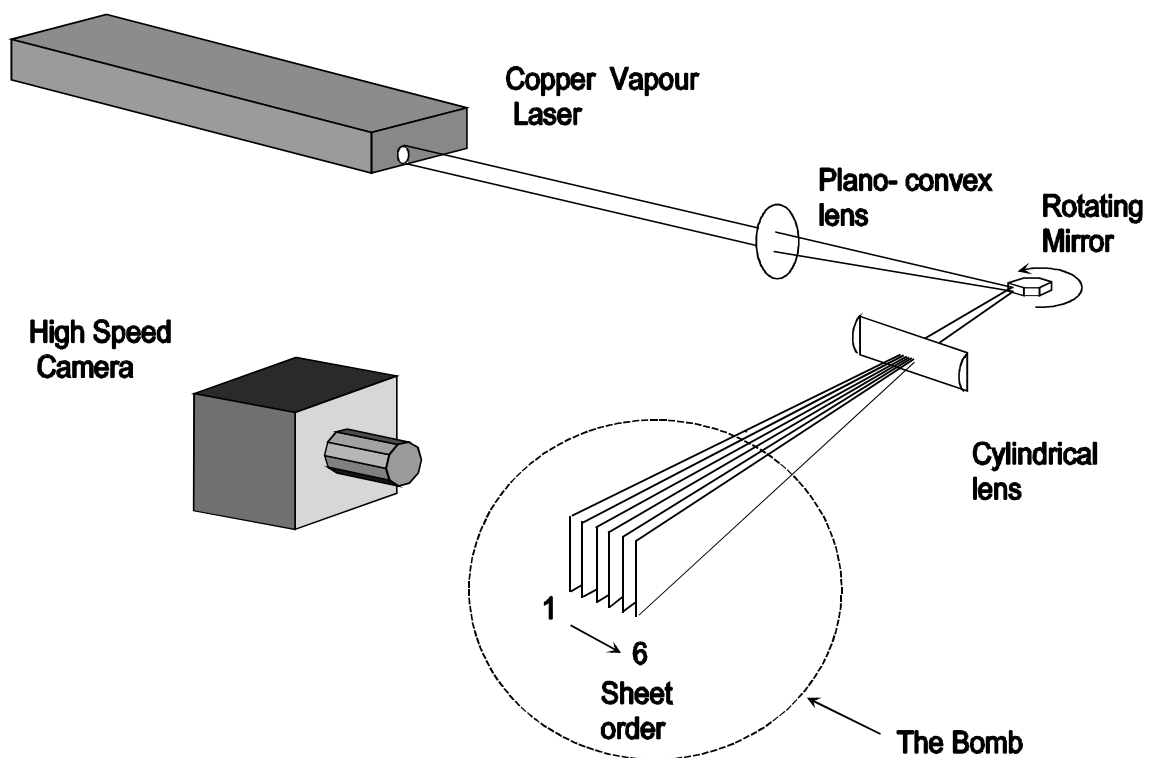


Figure 1. Schematic diagram of the experiment.



Figure 2. Twenty five “slices” through a methane-air flame at “one instant”, $\phi=0.6$, $u_f=0.09$ m/s, $u' = 0.56$ m/s and 28.9 ms from ignition. Separation of 0.7 mm between the images.

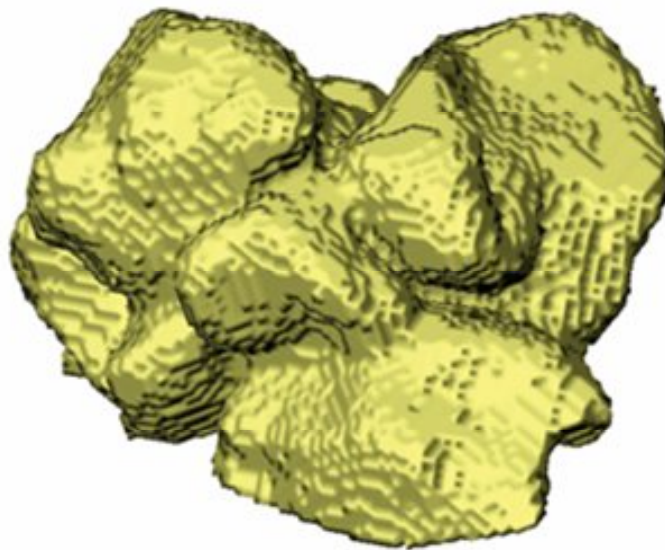


Figure 3. Typical image of a reconstructed flame after surface smoothing.

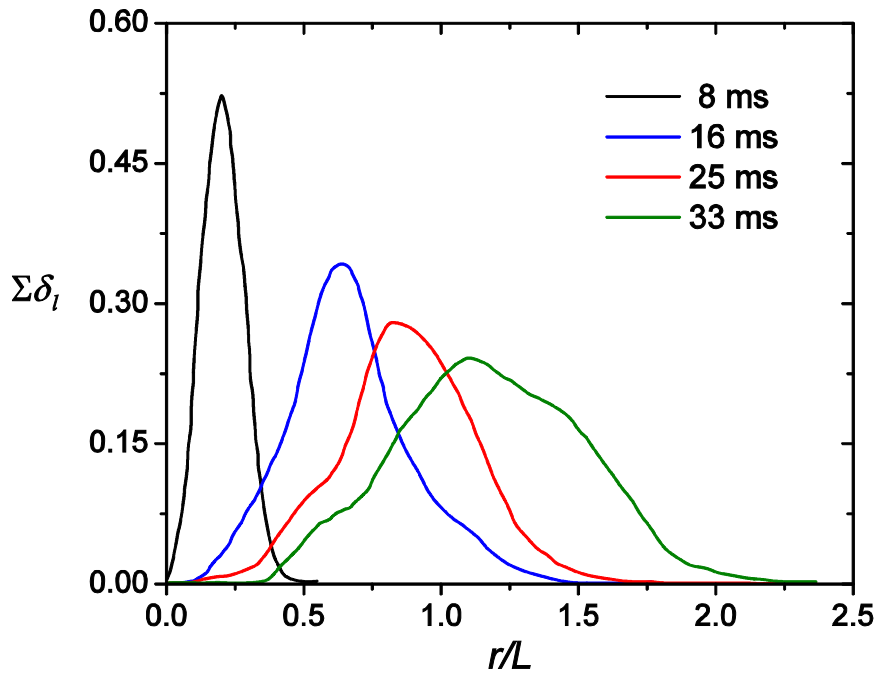


Figure 4. Variation of average normalised flame surface density ($\Sigma\delta_t$) with normalised radius (r/L) for methane-air flame, $\phi=0.7$, $u_t=0.16$ m/s and $u'=0.4$ m/s at different times after ignition.

6. References

- [1] Abdel-Gayed RG et al. (1987). Turbulent burning velocities: a general correlation in terms of straining rates. Proc. R. Soc. Lond. A 414: 389.
- [2] Gillespie L et al. (2000). Aspects of laminar and turbulent burning velocity relevant to SI engines. SAE paper 2000-01-0192.
- [3] Hicks RA et al. (1994). Multiple laser sheet imaging investigation of turbulent flame structure in a spark ignition engine. SAE paper 941992.
- [4] Lee TW et al. (1993). Surface properties of turbulent premixed propane/air flames at various Lewis numbers. Combust. Flame. 93: 445.
- [5] Chew TC et al. (1990). Spatially resolved flamelet statistics for reaction rate modeling. Combust. Flame. 80: 65.
- [6] Yip B et al. (1987). Time-resolved three-dimensional concentration measurements in a gas jet. Science. 235: 1209.
- [7] Bradley D et al. (1996). Study of turbulence and combustion interaction: Measurement and prediction of the rate of turbulent burning. Technical Report, University of Leeds, Leeds, UK.
- [8] Taubin G. (1995). A signal processing approach to fair surface design. Proceedings of the Fifth International Conference on Computer Vision, Washington DC, USA. IEEE Computer Society. ISBN 0-8186-7042-8.
- [9] Gashi S et al. (2005). Curvature and wrinkling of premixed flame kernels-comparisons of OH PLIF and DNS data. Proc. Combust. Inst. 30: 809.